

## Optical Neuro-Computing

Eung Gi Paek

*Bellcore 331 Newman Spring Road Red Bank, New Jersey 07701*

(Received: September 15, 1991)

In this paper, we review a new type of optical computing-optical neuro-computing-which was inspired to emulate the computational capability of the human brain. Also, recent activities at Bellcore for the implementation of optical neuro-computers are described.

### I. INTRODUCTION

The recent increased activity in implementing neural network<sup>[1-3]</sup> is mainly due to the potential of neural computers to mimic the computational ability of humans. Optics, especially coherent optics, is promising in implementing neural network models especially for 2D images because the operation is fully parallel along both x and y directions, and analog. Moreover, optics provides a large number of available neurons, typically a million. Many neurons in one layer can be connected into those in another layer through free space along the third dimension, eliminating the need for physical point-to-point connections. Finally, the wave nature of optics gives certain powerful computations, such as Fourier transform, convolution, correlation and so on, which are crucial in neural network implementations. Many systems utilizing the advantages of optics have been demonstrated.<sup>[4-15]</sup>

However, the systems based on coherent optics require bulky optics and critical alignments, making the systems impractical. In this paper, we will focus on this issue of compactization of coherent optical neuro-computers by taking two typical holographic neuro-processors, a holographic word-break recognizer and an on-line learning machine, as examples.

### II. HOLOGRAPHIC ASSOCIATIVE MEMORY FOR WORD-BREAK RECOGNITION

As a first example of optical neuro-processors, we describe a special type of associative memory for "word-break" problem.<sup>[16]</sup> The problem can be illustrated in the following sentence:

#### **Text Reeding Without Word Brecks May Became Difficult**

Without spaces between words, it is difficult to decipher the text. The task becomes even more difficult if the words each of which is embedded in a continuous stream of other letters, correct errors in the words, and insert spaces between them. The system must be shift invariant so that an input word can be recognized in any position. Since many words appear at the input window simultaneously, the system should also be able to process multiple inputs without crosstalk. Moreover, the system should be able to insert word-breaks at suitable positions between words.

By modifying a Hopfield-style holographic associative memory<sup>[9]</sup> to include the various features described above, a holographic word-break recognizer has been demonstrated.<sup>[17]</sup> As shown in Fig. 1, memory words are stored in a conventional Fourier transform hologram. The recognition part of the system consists mainly of a holographic VanderLugt correlator.<sup>[18]</sup> For word-break recognition, the input word stream is presented at the input plane of the system. Autocorrelation peaks that appear at places where there is a match between the input and memory are detected and the

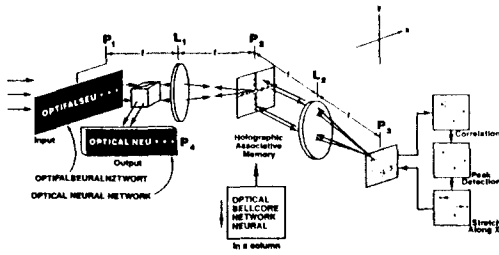


Fig. 1. Schematic diagram of the holographic word-break recognition system.

separation between the peaks magnified along the word direction. This stretched correlation output is reflected back to illuminate the hologram and reconstruct the whole memory at the output plane. The output through a window which is situated at the origin of the output plane is the desirable readable text. Fig. 2 shows the experimental results. The four words used as the memories in this experiment are shown in Fig. 2 (a). The concatenated input with errors is shown in (b). The correlation output is shown in (c). The sharp autocorrelation peaks appear at the corresponding positions of the input words and memories. Also, sidelobes appear over the whole correlation plane. Fig. 2(d) shows the thresholded and anamorphically magnified version of the correlation output. The final output from the system is shown in Fig. 2(e). Compared with the initial input in (b), spaces are inserted between words and all the errors in the input are corrected.

### III. HOLOGRAPHIC LEARNING MACHINE FOR MULTICATEGORY CLASSIFICATION

As a second example of optical neuro-processors, we describe a holographic on-line learning machine that can be trained to read characters the same way as a child does.<sup>19</sup> Fig. 3 shows a diagram of the experimental optical learning machine for multicategory classification. Each of the input training patterns, stored on a OMDR (optical memory disc recorder) is loaded onto a two-dimensional spatial light modulator (Hughes liquid crystal light valve) using a monitor and the lens,  $L_1$ . The loaded image is read out by a collimated coherent beam from an Argon laser and

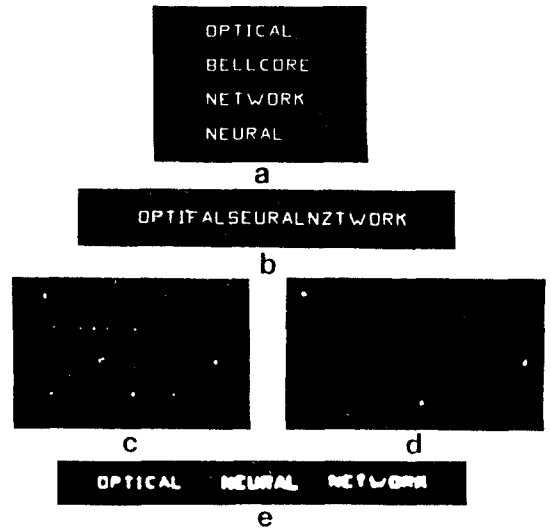


Fig. 2. (a) The four patterns stored in the holographic memory; (b) The input to be read; (c) correlation output; (d) the thresholded version of the correlation output which is anamorphically magnified along the x (word) direction; and (e) the associative recalled output with spaces between words and error corrections.

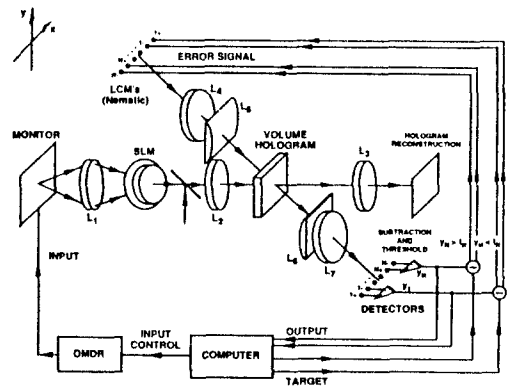


Fig. 3. Schematic of the holographic learning machine for multicategory classification.

is focused onto a photorefractive crystal (0.01% iron-doped  $\text{LiNbO}_3$ ) using the lens,  $L_2$ . The light diffracted from the photorefractive crystal is collected and focused onto a detector array. The detector array, which is located at the image plane of the LCM (liquid crystal modulator) array, consists of 20 detector elements to

represent the bipolar (+ and -) values for ten outputs. The outputs from each pair of detectors are subtracted, thresholded and latched. The error signals are generated by comparing the output with the desired target signals. The error signals thus obtained are loaded to an array of 20 LCM's to represent 10 bipolar error values. We fabricated a twisted nematic liquid crystal array specifically for this experiment. The light from the LCM array is focused to the photorefractive crystal and interferes with the input to reconfigure the information recorded on the crystal. The interconnection strengths recorded on the hologram can be read out by the light from each element of the LCM and can be externally stored and reloaded at a later time.

Fig. 4 shows a typical experimental learning curve (number of errors vs. iteration) obtained from the systems for 24 training patterns as shown in Fig. 4(a). The number of errors is summed for all the output neurons (both positive and negative neurons) and for all memories. Therefore, the number of maximum possible errors is  $M^2$ , where M represents the number of images in the training set. Initial conditions of the interconnection strengths are arbitrarily determined to small random numbers mostly due to background noise, scattering from the crystal, and the non-uniformity of the detector array. Characters of three different sizes and orientation are trained to be classified into one of eight output states. As shown in Fig. 4(b), the

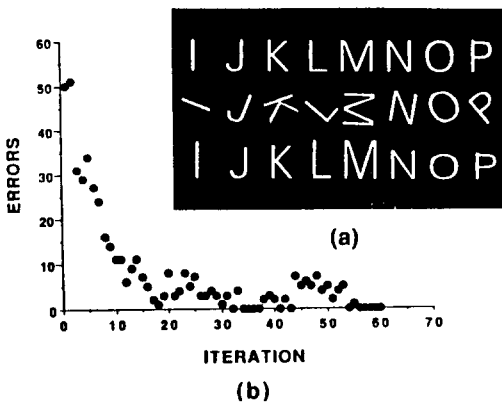


Fig. 4. (a) 24 training patterns and (b) experimental learning curves.

system successfully converged to the no error state after 55 iterations, even though the training sets are far from being orthogonal.

#### IV. A COMPACT HOLOGRAPHIC ON-LINE LEARNING MACHINE

The holographic on-line learning machine described above is very attractive and promising because the advantages of optics can be fully utilized. However, the system requires bulky optical components and critical alignment. Therefore, it is difficult to cascade the system to implement a multilayer network. It should be noted that the shift property of the optical Fourier system was not utilized in the present system shown in Fig. 3. Since a volume hologram is used, one cannot expect shift invariant recognition because of the phase matching selection of volume holograms. This relaxes the system requirements significantly. The only conditions the system has to satisfy are: Both input and error signals have to interact globally inside the photorefractive crystal, and the LCM array has to be imaged on the detector array. The reason we had to use many optical components in our system to focus light in the medium was because of the low sensitivity of the photorefractive crystal. If the sensitivity of the photorefractive crystal is high enough, the system can be significantly simplified as in Fig. 5.<sup>[20]</sup> Input and error spatial light modulators are directly attached on the photorefractive crystal. To ensure global interaction between the input and error inside the photorefractive crystal,

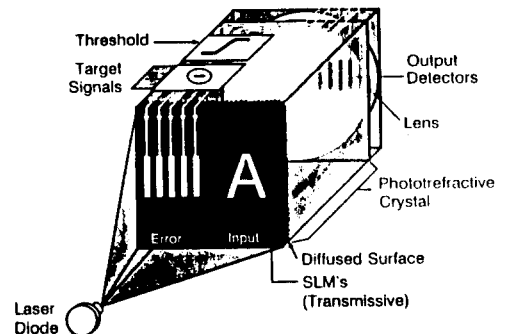


Fig. 5. A compact holographic on-line learning machine.

a diffuser is inserted between the spatial light modulator and the photorefractive crystal. An unpolished surface of the crystal can work as a diffuser also. At the other end of the crystal, a lens and a detector array are attached. Instead of cementing a lens on the photorefractive crystal, the refractive index of the crystal can be changed by ion implantation, modifying the optical power. In this way, a compact and robust holographic learning machine that does not require any alignment can be implemented. If ideal nonlinear optical devices are available in the future, even the feedback loop can also possibly be achieved optically.

### V. COMPACT HOLOGRAPHIC ASSOCIATIVE MEMORY USING A SURFACE-EMITTING MICRO-LASERARRAY

Now, we will demonstrate another example of compactization of optical neuro-processors by taking the associative memory for word-break problem as an example. Recently, low-threshold electrically pumped vertical-cavity surface-emitting microlaser diode arrays (SELDA's) have been reported.<sup>[21,22]</sup> The SELDA's have many features that make them highly desirable for use in holographic memory systems. The individual lasers can be as small as a few microns, allowing over one million microlasers on a 1 cm<sup>2</sup> chip. The wavelength of the light from the laser is 960 nm with the linewidth of around 0.1 nm. This gives a coherence length of several cm and a spectral resolution of about 10,000. Therefore a hologram of a high resolution image can be recorded and reconstructed by using an SEL. The threshold current of the laser is low, around 1 mA for lasers less than 5 μm in diameter, keeping device power requirements down. The output optical power from these lasers can be more than 100 mW depending on size. Therefore the light from each laser is bright enough to reconstruct a hologram which can be detected by a normal 2D image sensor. The lasers exhibit high switching speeds (less than 1 nanosecond) allowing fast optical access and proving very high contrast since an OFF laser generates no light. So, the question is how to utilize the novel device for optical neuro-processing. In the following we will de-

monstrate how the associative memory described above can be made compact using the SELDA. We note that the associative memory consists of two parts: the first part is a pattern recognizer to compare an input with the memories stored in a holographic memory and the second part is the reconstruction part to retrieve the corresponding memory on the output plane.

#### 1. A Compact and Ultra-Fast Holographic Memory

We describe a compact and ultra-fast holographic read-only memory that eliminates the need for a bulky laser, SLM's or beam steering optics by using the SELDA. As explicitly shown in Fig. 6, a SELDA combined with a simple collimating lens works as a very efficient multiple beam steerer to change the beam direction to reconstruct holographic memories. By using this simple and compact optical setup, any frame can be randomly accessed in less than 1 nanosecond (without considering detection time).

In the experimental results shown in Fig. 7, memo-

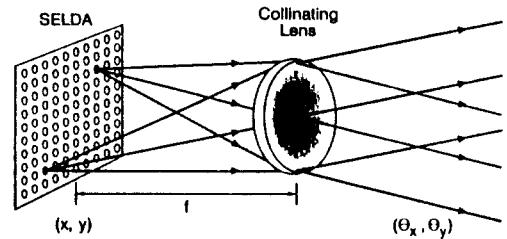


Fig. 6. Multiple beam steering using surface-emitting micro-laser arrays.

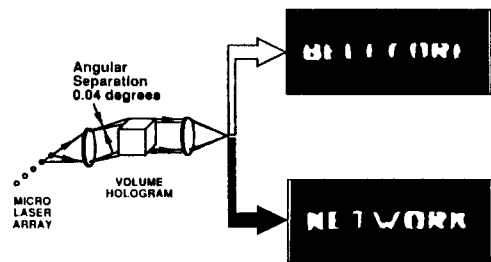


Fig. 7. A compact and ultra-fast volume holographic memory using a SELDA.

ries are recorded in a volume hologram (LiNbO<sub>3</sub> crystal, 0.01% Fe doped LiNbO<sub>3</sub>, 20×20×7 mm<sup>3</sup>, Deltronic Co.) which can provide a large storage capacity up to 10<sup>10</sup> (theoretically 10<sup>12</sup>) using the third dimension available in a volume storage medium.<sup>[23,23]</sup> Fig. 7 shows the reconstructed images from the volume hologram by using the light from a SELDA. Each laser is separated from the adjacent one by 70 μm, corresponding to an angular separation of about 0.04 degree which corresponds to 0.02 degree for the recording wavelength. As can be seen in the Figure, the two independent lasers separated by about 0.04 degree reconstruct totally different images. In this way, each microlaser can be matched to a separate page, allowing the array to form a selective address generator.

**2. A Compact and Robust Holographic Correlator**

Next, we will show that the recognition part of the associative memory shown in Fig. 1 can also be characterized using the SELDA. As mentioned previously, spectral linewidth of the light from a surface-emitting laser (SEL) is very narrow, allowing extremely high temporal coherence. However, the phase of the light from each of the SEL is not locked with each other i.e., the lasers are spatially incoherent. These two unique coherence properties (temporally highly coherent and spatially incoherent) make a SELDA and ideal light source in implementing a compact and robust incoherent correlator.<sup>[25]</sup>

Fig. 8 shows an incoherent correlator using a SE-

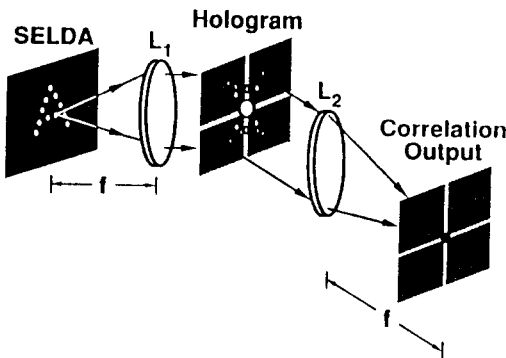


Fig. 8. A compact and robust 2D correlator using a SELDA.

LDA. The light from each of the SELDA is collimated by the lens, L<sub>1</sub> and illuminates the hologram to reconstruct holographic images on the output plane which is located at the focal plane of the lens, L<sub>2</sub>. The image generated by each SEL is shifted by the amount corresponding to the position of the SEL. The reconstructed images generated by the light from different SEL's are added up incoherently because each laser operates independently, averaging out the phase-sensitive interference terms. The eventual summation of all the reconstructed images generated by all the SEL's in the input plane gives the correlation between the input and the reference image stored on the hologram.

In such an incoherent correlator, the hologram need not be separated from the adjacent two lenses, L<sub>1</sub> and L<sub>2</sub> by the focal lengths and even can be in contact, reducing the physical of the system. Since the system does not involve any moving parts (e.g., rotating diffuser) or bulky optical components, the whole system can be miniaturized and integrated using semiconductor technologies.

Fig. 9 shows the correlation output obtained from the SELDA correlator. A holographic filter was fabricated for the input pattern, Bell logo, and was tested for the two input patterns, Bell and Chinese character meaning 'light'. These two input patterns are shown at the top of the Figure. Figures at the bottom show the correlation outputs for the corresponding inputs shown at the top. For the correct input, Bell, a bright autocorrelation peak appears at the center of the correlation output (bottom left). For the incorrect input, Chinese character, a crosscorrelation is obtained (bot-

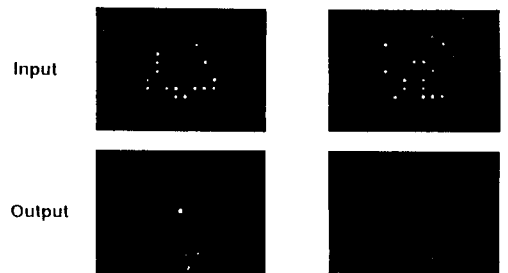


Fig. 9. Correlation outputs from the SELDA correlator. Inputs (top) and correlation outputs (bottom) for the holographic filter for a Bell logo.

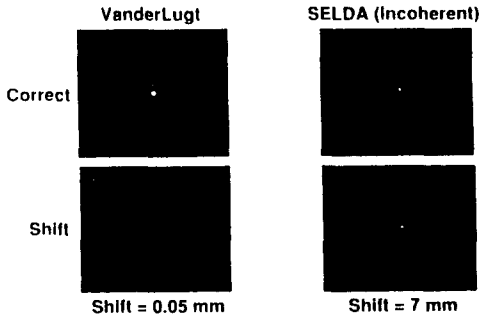


Fig. 10. Filter positioning tolerances of a VanderLugt correlator (left) and the SELDA correlator (right).

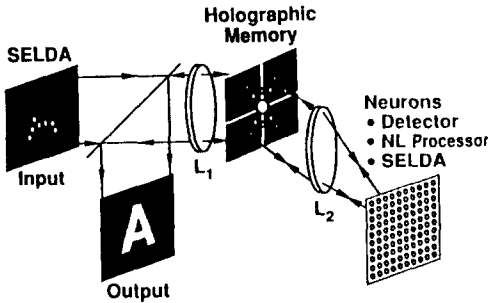


Fig. 11. Compact and robust holographic associative memory.

tom right). As shown in the Figure, the crosscorrelation signal is much weaker than the autocorrelation peak, allowing a satisfactory discrimination between the two input patterns.

Fig. 10 compares the filter positioning tolerance of the SELDA correlator with that of a vanderLugt correlator. In case of a VanderLugt correlator, a sharp autocorrelation peak is obtained as shown in the Figure (top left). However, after disturbing the filter by only  $50 \mu\text{m}$ , the recognition peak is completely lost. On the other hand, in case of the SELDA correlator, the correlation output is not noticeably affected even for the shift of the filter by 7 mm, demonstrating the robustness of the system.

### 3. A Compact and Robust Holographic Neuro-Processor

The correlator demonstrated above can be easily co-

mbined with the holographic memory system described in 1. using the same optical setup based on a two lens system. In the proposed system shown in Fig. 11, the light propagating from left to right calculates the correlations between the input and the memories stored on the hologram. The correlation outputs are thresholded by an array of optical nonlinear elements (optical neurons) and is reflected back to illuminate the hologram and retrieve the corresponding memory on the output plane. Due to the compactness and integrability of the system, it can be cascaded to implement even more complicated multilayer networks<sup>[17]</sup> using semiconductor technology.

## VI. CONCLUSION

In conclusion, we have shown that coherent optics is powerful in implementing various neural network models for two dimensional images. By using the recently developed surface emitting micro-laser diode array, the coherent optical systems can be made compact and robust, still preserving the power of coherent optics.

## REFERENCES

- [1] J. J. Hopfield, "Neural networks and Physical Systems with Emergent Collective Computational Abilities," Proc. Natl. Acad. Sci. U.S.A. **79**, pp. 2554-2558 (1982).
- [2] F. Rosenblatt, *Cornell Aeronaut. Lab. Report*, 85-460-1, 1957.
- [3] D. E. Rumelhart and J. L. McClelland, *Parallel Distributed Processing*, Cambridge, MA: M.I.T. (1986).
- [4] N. H. Farhat, D. Psaltis, A. Prasad and Eung Gi Paek, "Optical Implementations of the Hopfield Model," Appl. Opt. **24**, 1496 (1985).
- [5] D. Psaltis and N. H. Farhat, "Optical information processing based on an associative-memory model of neural nets with thresholding and feedback," Opt. Lett. **10**, 98 (1985).
- [6] B. H. Soffer, G. H. Dunning, Y. Owechko and E. Marom, "Associative holographic memory with feedback using phase-conjugating mirrors," Opt. Lett. **11**, 118 (1986).
- [7] D. Anderson, "Coherent optical eigenstate me-

- mory," *Opt. Lett.* **11**, 56 (1986).
- [8] A. Yariv, S. K. Kwong and K. Kyuma, "Optical associative memories based on photorefractive oscillations," *Proc. SPIE*, **613**, 1 (1986).
- [9] E. G. Paek and D. Psaltis, "Optical associative memory using Fourier transform holograms," *Opt. Eng.* **26**, 428 (1987).
- [10] J. S. Jang, S. W. Jung, S. Y. Lee and S. Y. Shin, "Optical implementation of the Hopfield model for two-dimensional associative memory," *Opt. Lett.* **13**, 248 (1988).
- [11] J. S. Jang, S. Y. Shin and S. Y. Lee, "Optical implementation of quadratic associative memory with outer-product storage," *Opt. Lett.* **13**, 693 (1988).
- [12] S. H. Song and S. S. Lee, "Properties of holographic associative memory prepared by the polarization encoding process," *Appl. Opt.* **27**(15), 3149 (1988).
- [13] Y. Nitta, J. Ohta, K. Mitsunaga, S. Tai and K. Kyuma, "Opto-electronic associative memory using an advanced optical neurochip," *Appl. Opt.* **30**(11), 1328 (1991).
- [14] Y. Oechko, "Nonlinear holographic associative memories," *IEEE J. Quantum Elec.* **25**(3), 619 (1989).
- [15] J. H. Hong, S. Campbell and P. Yeh, "Optical pattern classifier with Perceptron learning," *Appl. Opt.* **29**, 20 (1990).
- [16] D. W. Tank and J. J. Hopfield, "Neural Computation by Concentrating Information in Time," *Proc. Nat. Acad. Sci.* 1896 (1987).
- [17] Eung Gi Paek and A. Von Lehmen, "Holographic Associative Memory for Word-break Recognition," *Opt. Lett.* **14**, 205 (1989).
- [18] A. VanderLugt, "Signal detection by complex spatial filtering," *IEEE Trans. Inform. Theory*, **IT-10**, 139 (1964).
- [19] Eung Gi Paek, J. R. Wullert II and J. S. Patel, "Holographic Learning Machine for Multi-category Classification," *Opt. Lett.* **23**, 1303 (1989).
- [20] Eung Gi Paek, J. R. Wullert II and J. S. Patel, "Holographic On-Line Learning Machine for Multicategory Classification," *Jap. J. Appl. Phys.* **29**, 1332 (1990).
- [21] J. L. Jewell, A. Scherer, S. L. McCall, Y. H. Lee, S. Walker, J. P. Harbison and L. T. Florez, "Low-Threshold Electrically Pumped Vertical-Cavity Surface-Emitting Microlasers," *Electron. Lett.* **2**(17), 1124 (1989).
- [22] Y. H. Lee, B. Tell, K. F. Brown-Geobeler, J. L. Jewell, and J. V. Hove, "Top-surface-emitting GaAs four-quantum-well lasers emitting at 0.85  $\mu\text{m}$ ," *Electron. Lett.*, **26**, 710 (1990).
- [23] Yu, N. Denisyuk, "Photographic Reconstruction of the Optical Properties of an Object in its Own Scattered Radiation Filled," *Sov. Phys. Dokl.* **7**, 543 (1962).
- [24] P. J. van Heerden, "Theory of Optical Information in Solids," *Appl. Opt.* **2**, 393 (1963).
- [25] Eung Gi Paek, John R. Wullert II, M. Jain, A. Von Lehmen, A. Scherer, J. Harbison, H. J. Yu and R. Martin, "A Compact and Ultra-Fast Holographic Memory Using a Surface Emitting Micro-Laser Diode Array," *Opt. Lett.* **15**, 341 (1990).
- [26] A. W. Lohmann, "Matched Filtering with Self-Luminous Objects," *Appl. Opt.* **7**, 561 (1968).